Synthesis, Spectroscopy, and Conductivity Studies of 4-(diphenylamino)benzaldehyde-4-(3-fluorophenyl) thiosemicarbazone and Their Metal Complexes

Sharmili Silvarajoo[1], Uwaisulqarni M. Osman[1,2*], Khadijah H. Kamarudin[1,2], Mohd Hasmizam Razali[1,2] and Mohd Zul Helmi Rozaini[3]

[1]Faculty of Science and Marine Environment, Universiti Malaysia Terengganu 21030 Kuala Nerus, Terengganu, Malaysia

[2]Advanced Nano Materials Research Group (ANOMA), Ionic State Analysis (ISA) Laboratory Universiti Malaysia Terengganu, 21030 Kuala Nerus, Terengganu, Malaysia

[3]Faculty of Fisheries and Food Science, Universiti Malaysia Terengganu, 21030 Kuala Nerus Terengganu, Malaysia

*****Corresponding author (e-mail: uwais@umt.edu.my)

This is a continuation of our previously published spectroscopy and conductivity studies of thiosemicarbazone derivatives. In this study, the 4-(diphenylamino)benzaldehyde-4-(3-fluorophenyl) thiosemicarbazone (LH) ligand was synthesized from the reaction between 4-diphenylamino-benzaldehyde and 3-fluorophenyl thiosemicarbazide. The NiL_2, CuL_2, and CoL_2 complexes containing the LH ligand were also synthesized and characterized by elemental analysis, infrared spectroscopy, magnetic susceptibility, molar conductivity and UV-Vis spectroscopy. The LH ligand was characterized *via* ^{1}H NMR and ^{13}C NMR spectroscopy. FTIR data was used to determine the coordination mode of the ligand with the Ni(II) metal ion. The FTIR spectra showed that LH behaved as a mononegative bidentate ligand with all metal ions, through its azomethine (N=C) and (C-S) groups. The electronic spectra and magnetic measurements suggest a square planar geometry for both the NiL_2 and CuL_2 complexes, with μ_{eff} values of 0.00 and 2.36 B.M, respectively. However, CoL_2 was likely to possess a tetrahedral geometry, with μ_{eff} = 4.02 B.M. All complexes displayed non-electrolytic behaviour with low molar conductance values in the range of 5.97 – 13.20 Ω^{-1} cm^2 mol^{-1}. Polymer electrolyte (PE) films were mixed with carboxymethyl cellulose (CMC) polymer, propylene carbonate as a plasticizer and the LH/NiL_2/CuL_2/CoL_2 compound as a dopant, and prepared using a solution casting technique. The conductivity of the prepared PE films was studied using Electrochemical Impedance Spectroscopy (EIS). The conductivity values observed for the LH ligand, NiL_2, CuL_2, and CoL_2 complexes were 5.58×10^{-8}, 7.72×10^{-8}, 9.58×10^{-7} and 3.10×10^{-8} S cm^{-1}, respectively. Thus, the presence of metal ions may affect the conductivity of polymer electrolytes.

Keywords: Thiosemicarbazone; metal complexes; spectroscopy; polymer electrolytes

Received: February 2023; Accepted: April 2023

Thiosemicarbazone is produced by a condensation reaction between thiosemicarbazide and an aldehyde or a ketone. Upon complexation, thiosemicarbazone binds to a metal ion through its nitrogen (N) and sulphur (S) donor atoms.

Currently, several synthesized compounds have been used as conductors such as coordination polymers [1], ceramic oxide [2] and metal-organic frameworks (MOFs) [3]. To design good conductor compounds, good inter- and intra-hydrogen bonding networks for efficient proton transfer and resistance at higher temperatures are crucial factors [4,5]. To achieve these conducting pathways, the incorporation of metal ions and the presence of donor atoms are very important. It is commonly believed that metal ions bind strongly to ligands, while slightly electronegative NS donor atoms attract slightly electropositive hydrogen atoms. Thus, it is better to design coordination compounds with metal complexes for proton transport.

In this work, new thiosemicarbazone derivatives with selected transition metal ions, namely Ni^{2+}, Co^{2+} and Cu^{2+}, were synthesized and characterized by various spectroscopic methods and thermal analysis. All these new compounds were evaluated for their potential conductivity using Cole-Cole plots.

EXPERIMENTAL

Chemicals and Materials

All chemicals were obtained commercially from various suppliers and used directly without any further

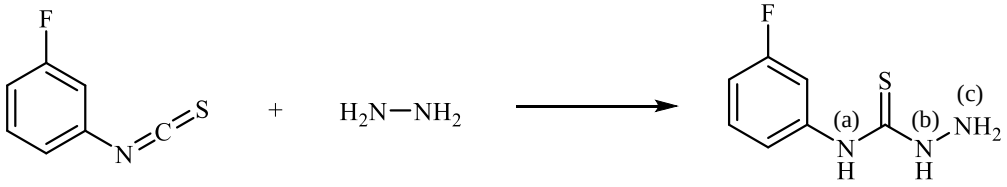

Scheme 1. Chemical equation for 3-fluorophenyl thiosemicarbazide (LH1).

purification. The reagents used were propylene carbonate (99.7%, Sigma Aldrich), hydrazine hydrate (Sigma Aldrich), 4-diphenylaminobenzaldehyde (Sigma Aldrich), nickel (II) acetate tetrahydrate (Sigma Aldrich), copper (II) acetate monohydrate (R&M), cobalt (II) acetate tetrahydrate (R&M), 3-fluorophenyl isothiocyanate (Alfa), glacial acetic acid (Emsure) and carboxymethyl cellulose, CMC (Acros Organic). The solvents used were absolute ethanol, 85% ethanol and methanol (Hamburg), acetonitrile (Emsure), distilled water, dimethylsulphoxide (R&M) and dimethylformamide (Fisher).

Characterization Methods

Synthesis of 3-fluorophenyl Isothiocyanate (LH1)

A mixture of 3-fluorophenyl isothiocyanate (1.22 mL, 0.01 mol) and hydrazine hydrate (0.31 mL, 0.01 mol) in ethanol was stirred in an ice bath for 1 hour using a mechanical stirrer. During this time, a cloudy solution was observed. The solution was then stirred at room temperature for 3 hours, and a white precipitate was formed. This solid was filtered, washed with cold ethanol, and recrystallized with methanol. The final product was kept in a desiccator. The chemical reaction for LA1 is shown in **Scheme 1**.

Synthesis of Schiff base, 4-(diphenylamino)benzalde hyde-4-(3-fluorophenyl)thiosemi-carbazone (LH2)

4-diphenylaminobenzaldehyde was placed in a two-neck round bottom flask for the reflux process. 0.185 g (0.001 mol) of 3-fluorophenyl thiosemicarbazide with 20 mL of methanol was added dropwise into the 4-diphenylaminobenzaldehyde solution, followed by five drops of glacial acetic acid. After the addition of 2-fluorophenylthiosemicarbazide, the mixture was stirred at room temperature and refluxed for 5 hours. The solution was then cooled at room temperature until a crude product was precipitated. This crude product was recrystallized from methanol to afford a yellow compound, LH2. The chemical reaction for LH2 is shown in **Scheme 2**.

Synthesis of Ni(II) Metal Complex, Ni(LH2)$_2$

The Schiff base, LH2 (0.180 g, 1x10^{-3} mol) was weighed and dissolved in hot ethanol (30 mL). This solution was stirred with a magnetic stirrer at 70 °C. Nickel(II) acetate tetrahydrate (0.124 g, 0.5x10^{-3} mol) was dissolved in 20 mL of hot ethanol in another beaker. The nickel (II) acetate solution was added dropwise into the LH2 solution and left stirring for 2 hours to ensure a homogeneous solution. During the heating process, a brownish precipitate was formed. The residue was then filtered and dried in the desiccator. The chemical reaction for Ni(LH2)$_2$ is shown in **Scheme 3**.

The same method was repeated with two other metal complexes, copper (II) acetate monohydrate and cobalt (II) acetate tetrahydrate, to form Cu(LH2)$_2$ and Co(LH2)$_2$, respectively.

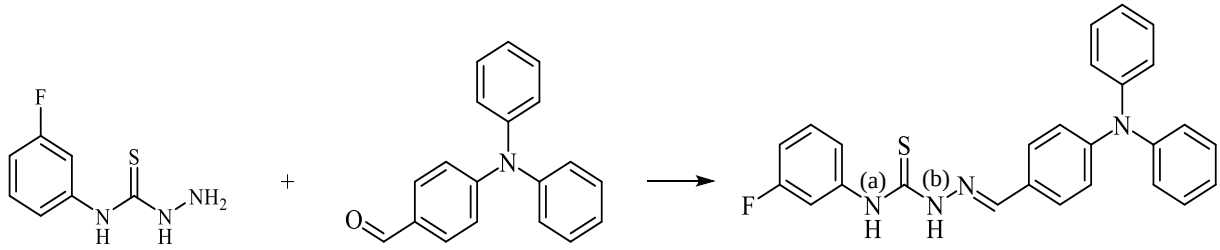

Scheme 2. Chemical equation for Schiff base, 4-(diphenylamino)benzaldehyde-4-(3-fluorophenyl)thiosemicarbazone (LH2)

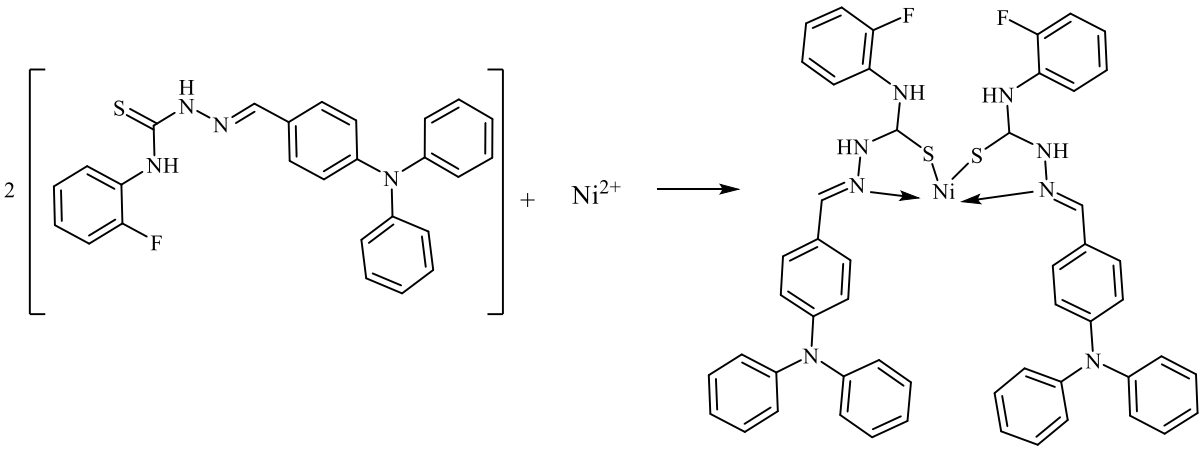

Scheme 3. Chemical equation for $Ni(LH2)_2$.

Preparation of Thin Film

Carboxymethyl cellulose (CMC) (1 g) was weighed and added to 20 mL of distilled water. The mixture was left to stir for one hour until it dissolved completely. In another beaker, 0.0475 g (15 wt%) of each compound and 0.026 g (8 wt%) propylene carbonate (PC) were dissolved in 30 mL of ethanol, and added dropwise into the CMC solution which was then kept in the oven at 60 °C overnight.

Electrochemical Impedance Spectroscopy

The polymer electrolyte (PE) films were cut into small discs of 2 cm diameter and sandwiched between two stainless steel electrodes under spring pressure. The measurements were carried out at room temperature (303 K). The conductivity of the PE films were calculated using Eq. 1 [6].

$$\sigma = \frac{t}{A \times R_b} \quad (1)$$

where t = thickness of PE film (cm)
A = surface contact area of PE film (cm^2)
R_b = bulk resistance of PE film (Ω)

RESULTS AND DISCUSSION

Characterization

The physical characteristics of the ligands and their transition metal complexes are shown in Table 1. All transition metal complexes had higher melting points than the free ligands, due to their higher molecular weights. The experimental and calculated values obtained from the CHN elemental analysis were close in agreement, with a maximum difference of 2.6 %. Thus, all the ligands and metal complexes were relatively free from impurities, except for $LH1.H_2O$. All complexes had a metal:ligand ratio of 1:2.

Table 1. Analytical data and physical properties of the ligands and their metal complexes.

Compound	Colour	Melting Point (°C)	Experimental value (Calc.)		
			%C	%H	%N
$LH1.H_2O$	White	170.7	38.17 (38.00)	4.79 (5.42)	20.28 (19.00)
LH2	Yellow	189.6	69.70 (70.90)	4.72 (4.77)	11.89 (12.73)
$Ni(L2)_2$	Brownish-green	278.6	65.29 (66.61)	4.36 (4.27)	11.13 (11.96)
$Cu(L2)_2$	Yellowish-green	204.4	65.98 (66.28)	4.29 (4.25)	11.68 (11.90)
$Co(L2)_2$	Brown	210.0	64.00 (66.60)	3.99 (4.27)	11.00 (11.95)

The IR spectral data for all ligands and their metal complexes are shown in Table 2. In LH1, the bands for ν(N-H_2), ν(N-H)^a, ν(N-H)^b and ν(C=S) were located at both 3254 and 3228, 3296, 3198, 1559 and both 1318 and 870 cm^{-1}, respectively. These are typical bands for thiosemicarbazide derivatives [6].

LH2 showed significant peaks at 1274, 3189, 1540 and 1136 cm^{-1}, corresponding to the ν(C-F), ν(N-H)^a, ν(N-H)^b, δ(N-H) and ν(N-N) functional groups, respectively. The disappearance of the ν(N-H_2) band in LH2 and the appearance of new bands attributable to ν(C-N) of triphenylamine confirmed the formation of thiosemicarbazone in LH2.

In addition, the LH2 compounds were expected to undergo thione-thiol tautomerism. However, the compounds were in thione form in the solid state. This was due to the presence of absorption peaks for the NH^b functional group at 3117 cm^{-1}. In addition, the C=S functional group was also observed at 1330 cm^{-1}. This confirmed that the compounds were in a thione tautomer solid state [7.8].

Based on the absorption of selected functional groups in the IR spectra, it may be concluded that LH2 coordinates to metal ions through its azomethine nitrogen and thiolate sulphur atoms. LH2 formed a thiol tautomer (C-SH) during deprotonation of SH to give a thiolate, whereas the proton in the (N-H)^b disappeared upon complexation.

In the IR spectra of all the metal complexes, the peak for the ν(N-H)^b functional group was missing due to the deprotonation of -SH by tautomerism [9]. The ν(CH=N) band shifted to a lower frequency (1580-1588 cm^{-1}) upon complexation, compared to 1594 cm^{-1} for the LH2 ligand. This evidence can be used to confirm that the metal ions had coordinated with the azomethine nitrogen [10]. Moreover, the thioamide bands ν(C=S) in the thiosemicarbazone derivative disappeared, and a new band attributable to ν(C-S) appeared at 678-681 cm^{-1} in the spectra of all the complexes. This is further supported by the occurrence of the other ν(N–N) band at higher frequencies in all the complexes due to the reduced repulsion force between the lone pair of electrons on the hydrazine nitrogen atoms [11]. Hence, the infrared spectra of the metal complexes confirmed they had coordinated with the ligands through the azomethine nitrogen and thiolate sulphur donor atoms.

Nuclear Magnetic Spectroscopy (NMR) Analysis of LH1 and LH2

The ^{1}H and ^{13}C NMR spectra for both LH1 and LH2 were recorded in DMSO-d_6 at 400 Hz, and the results are tabulated in Table 3.

The ^{1}H NMR spectrum for LH1 showed singlet peaks for NH^a and NH^b at δ_H = 7.84 and 9.29 ppm, respectively. A broad singlet absorption for NH_2 was observed at δ_H = 4.91 ppm. All protons in the phenyl ring were observed as multiplets in the range of δ_H =6.92-7.43 ppm.

The ^{1}H NMR spectrum of LH2 showed a singlet at δ_H = 10.06 ppm due to NH^a, while the signal at δ_H = 11.88 ppm can be assigned to the NH^b proton. The NH^b groups had shifted far downfield due to the electronegative azomethine nitrogen and sulphur atoms. A signal for the thiol group (-SH) proton was not observed at 4 ppm. This confirmed that LH2 existed in the thione form in DMSO-d_6 solution. This has also been observed with other thiosemicarbazone derivatives compounds [12].

A new peak for azomethine nitrogen, HC=N, appeared as a singlet peak at δ_H = 8.10 ppm in the spectrum of LH2, but this was not observed with LH1. This confirmed the formation of LH2, which has triphenylamine moiety. The peaks of the phenyl ring protons (H_{phenyl}) for the triphenylamine moiety in LH2 were observed in the normal range of δ_H = 6.91-7.76 ppm. This has also been noted by previous researchers [13].

Table 2. Infrared spectral data (cm^{-1}) of ligands and their metal complexes.

Compound	Band (Wavenumber, cm^{-1})									
	ν(C-F)	ν(N-H_2)	ν(N-H)^a	ν(N-H)^b	δ(N-H)	ν(N-N)	ν(C=S)	ν(C-S)	ν(CH=N)	ν(C-N)
LH1.H_2O	1276	3254, 3228	3296	3198	1559	1141	1318, 870	-	-	-
LH2	1274	-	3189	3117	1540	1136	1330, 872	-	1594	1189
Ni$(L2)_2$	1278	-	3317		1540	1173	-	681	1588	1230
Cu$(L2)_2$	1276	-	3359		1547	1174	-	681	1580	1231
Co$(L2)_2$	1276	-	3312		1532	1172	-	678	1585	1227

Table 3. ^{1}H NMR data for LH1 and LH2.

Compound	Chemical Shift δ_H (ppm)	Moiety
LH1	9.29	(s, 1H, NH^b)
	7.84	(s, 1H, NH^a)
	7.43-6.97	(m, 4H, C_6H_4)
	4.91	(s, 1H, NH_2)
LH2	11.88	(s, 1H, NH^b)
	10.06	(s, 1H, NH^a)
	8.10	(s, 1H, CH=N)
	7.76-7.78	(d, J=8.8Hz, 2H, C_6H_4)
	7.62-7.66	(dt, J=11Hz, 2Hz, 1H, C_6H_4)
	7.46-7.48	(m, 1H, C_6H_4)
	7.34-7.39	(m, 5H, C_6H_5/ C6H4)
	7.08-7.14	(m, 6H, C_6H_5/ C_6H_4)
	6.99-7.04	(m, 1H, C_6H_4)
	6.91-6.94	(d, J=8.8Hz, 2H, C_6H_5)

Table 4. ^{13}C NMR data for LH1 and LH2.

Compound	Chemical Shift, δc (ppm)	Moiety
LH1	179.54	C=S
	163.21, 160.81	C-F
	110.21-141.58	$C=C_{Ar}$
LH2	175.77	C=S
	163.15, 160.75	C-F
	111.93-129.99	$C=C_{ar}$
	149.54	CH=N
	143.58, 146.93	$C\text{-}N_{Triphenylamine}$
	121.58-141.33	$C=C_{Triphenylamine\ (Ar)}$

In the ^{13}C NMR data given in Table 4, the most downfield signals for both LH1 and LH2 ligands, at δ_C = 179.54 and 175.77 ppm, were assigned to the thiocarbonyl carbon, C=S. This result supported the theory that all the thiosemicarbazone derivatives were in thione form, even in solution. The new chemical shift for LH2 at 149.54 ppm was attributed to C=N. This peak can be used as evidence for the formation of LH2. The most crucial evidence would be the signal of a carbon atom bonded directly to a fluorine atom, where the aromatic carbon signal should split into a doublet when coupled with fluorine. However, the carbon coupled to fluorine did not split into a doublet as its coupling constant ^{4}J = 0 Hz [14].

UV-Vis Spectroscopic Analyses for All Compounds

The UV-Vis spectra (1 x 10^{-5} M) results for the ligands and their metal complexes are summarized in Table 5. The UV-Vis spectra for LH1 showed peaks at both 272.0 nm and 344.5 nm due to the π→π* and n→π* transitions, respectively. These transitions correspond to the aromatic ring and thione chromophore [15]. In the thiosemicarbazone derivative LH2, absorption bands were observed at 299.5 nm and 383.5 nm due to the π→π* and n→π* transitions, respectively. These peaks correspond to the presence of the triphenyl-amine core, aromatic ring, azomethine and thioamide chromophores [16,17].

In the spectra of all complexes, the bands for both π→π* (C=C) and n→π* (C=S, C=N) transitions were observed. The n→π* transition exhibited a hypsochromic shift at 299.0-325.0 nm due to the donation of a lone pair from the azomethine nitrogen to the central metal ion. These bands had shifted to higher or lower wavelengths compared to their corresponding free ligands [18].

In addition, the electronic spectra of all the complexes showed ligand-to-metal charge transfer (LCMT) bands at 364.0-406.0 nm, due to either a nitrogen to metal transition or a sulphur to metal transition (N → M and S → M). This indicates that the metal (II) ion was coordinated with the azomethine nitrogen and sulphur through the thiolo sulphur atom [19].

In the spectrum for both $Cu(L2)_2$ and $Ni(L2)_2$ complexes, shoulder bands at 453.0 and 779.0 nm were observed that corresponded to the $^1A_{1g} \rightarrow {}^1A_{2g}$ and $^2B_{1g} \rightarrow {}^2A_{1g}$ transitions, respectively, consistent with a square planar geometry [20]. However, the $Co(L2)_2$ complex exhibited a band at 750.0 nm due to the $^4A_2(F) \rightarrow {}^4T_1(F)$ transition, which implies a tetrahedral geometry [21].

Molar Conductance and Magnetic Data of the Metal Complexes Containing Thiosemicarbazone

Molar conductance and magnetic susceptibility measurements of the complexes were carried out in DMSO at a concentration of 1 x 10^{-3} M, and the results are listed in Table 6. The low molar conductance values (5.45-13.20 Ω^{-1} cm^2 mol^{-1}) indicate that all the complexes displayed non-electrolytic behaviour. These values are lower than those previously reported [22]. Thus, the non-electrolytic nature of the complexes proved that all the metal complexes were free of acetate anions.

Based on the magnetic susceptibility measurements, the $Ni(LB2)_2$ complex did not exhibit values consistent with diamagnetic properties, thus the $Ni(LB2)_2$ complex is likely to have a square planar geometry [23]. The $Cu(LB2)_2$ complex with a d^9 electron configuration had an μ_{eff} value of 2.36 B.M. This corresponds to the one unpaired electron and is in the normal range for a square planar Cu(II) ion [11,17]. However, the magnetic susceptibility of the $Co(LB2)_2$ complex was 4.20 B.M., which indicates a tetrahedral geometry [21,24].

Table 5. UV-Vis spectral (1 x 10^{-5} M) data of the ligands and their metal complexes.

Compound	Electronic spectral band (nm)	Assignment
LH1	272.0, 344.5	$\pi \rightarrow \pi^*$, $n \rightarrow \pi^*$
LH2	299.5, 383.5	$\pi \rightarrow \pi^*$, $n \rightarrow \pi^*$
$Ni(L2)_2$	283.0, 330.0 410.0, 453.0	$\pi \rightarrow \pi^*$, $n \rightarrow \pi^*$, L → M, $^1A_{1g} \rightarrow {}^1A_{2g}$
$Cu(L2)_2$	298.5, 325.0, 410.0, 779.0	$\pi \rightarrow \pi^*$, $n \rightarrow \pi^*$, L → M, $^2B_{1g} \rightarrow {}^2A_{1g}$
$Co(L2)_2$	299.0, 406.0, 750.0	$n \rightarrow \pi^*$, L → M, $^4A_2(F) \rightarrow {}^4T_1(F)$

Table 6. Molar conductance and magnetic susceptibility measurements of the metal complexes.

Compound	μ_{eff} (B.M.)	Molar conductance (Ω^{-1} cm^2 mol^{-1})
$Ni(LB2)_2$	0.00	5.97
$Cu(LB2)_2$	2.36	12.10
$Co(LB2)_2$	4.02	13.20

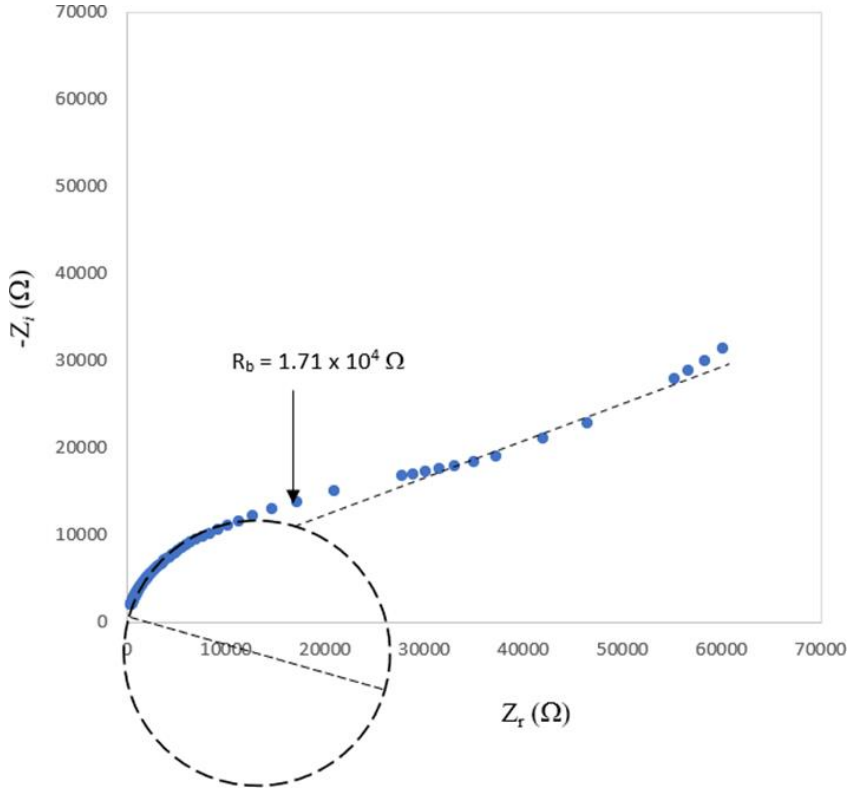
70000
60000
50000
40000
30000
20000
10000
0
-Z_i (Ω)
R_b = 1.71 x 10^4 Ω
0
10000
20000
30000
40000
50000
60000
70000
Z_r (Ω)

(a)

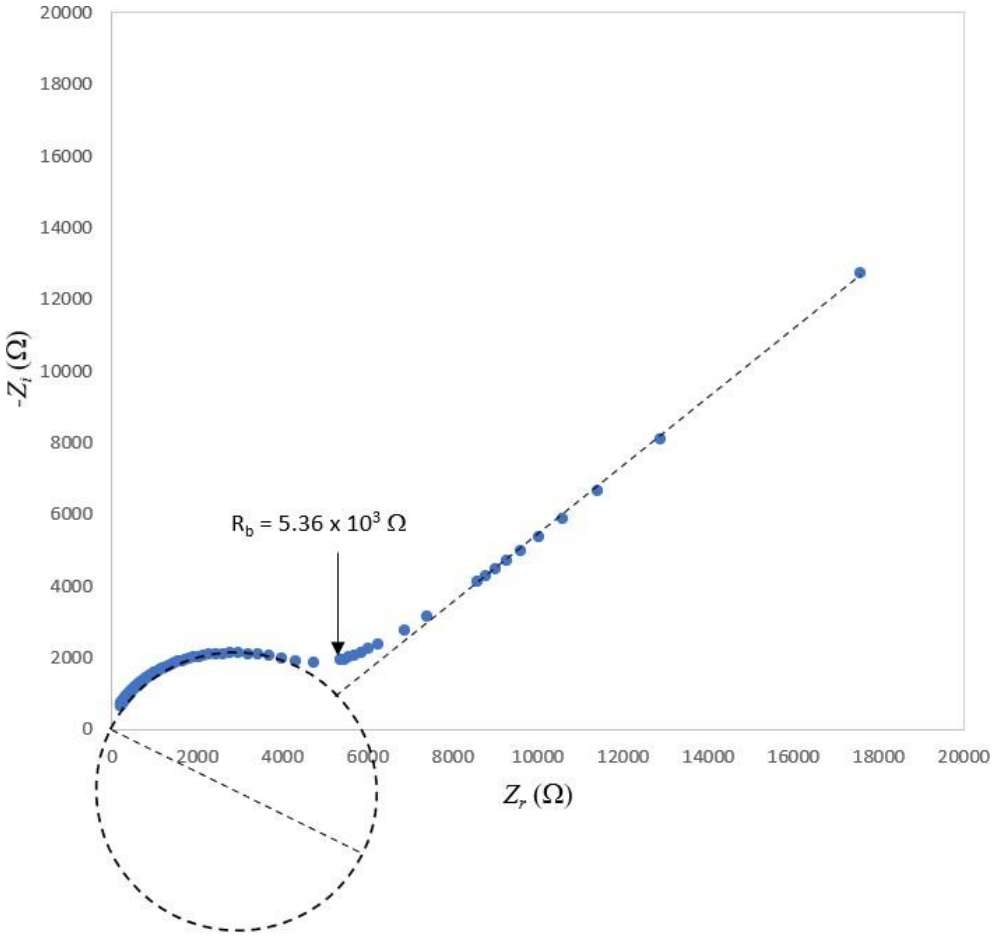
20000
18000
16000
14000
12000
10000
8000
6000
4000
2000
0
-Z_i (Ω)
R_b = 5.36 x 10^3 Ω
0
2000
4000
6000
8000
10000
12000
14000
16000
18000
20000
Z_r (Ω)

(b)

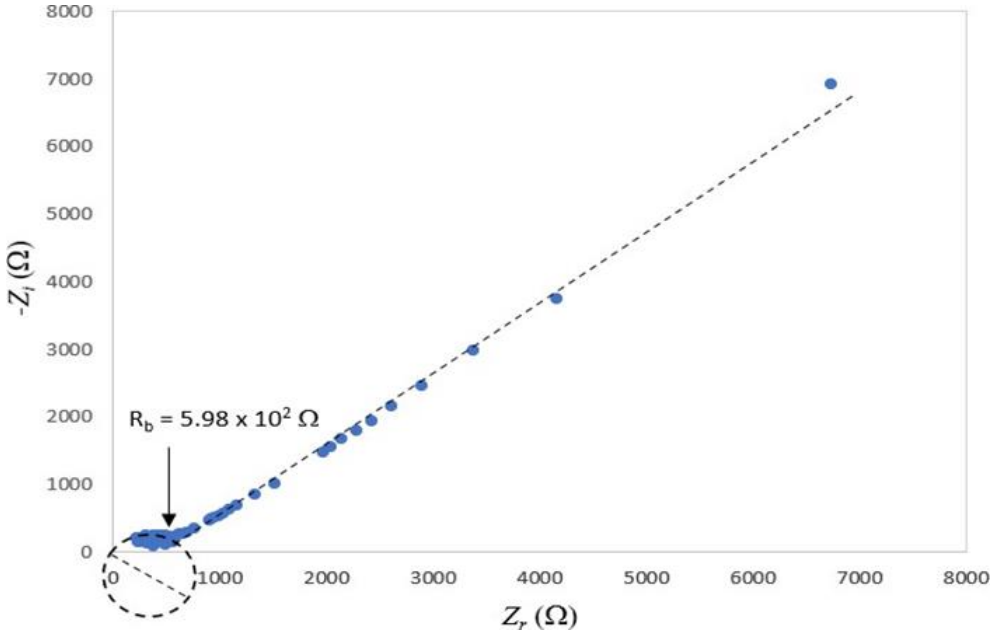

(c)

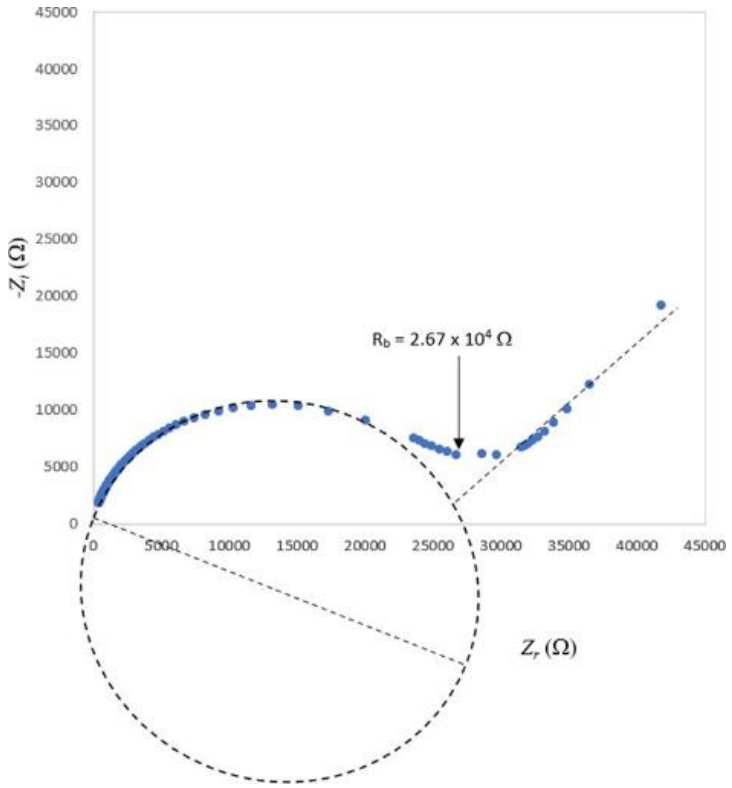

(d)

Figure 1. Cole-Cole plots for the thin films of (a) CMC-PC-LH2 (b) CMC-PC-[$Ni(LH2)_2$] (c) CMC-PC-[$Co(LH2)_2$], and (d) CMC-PC-[$Cu(LH2)_2$].

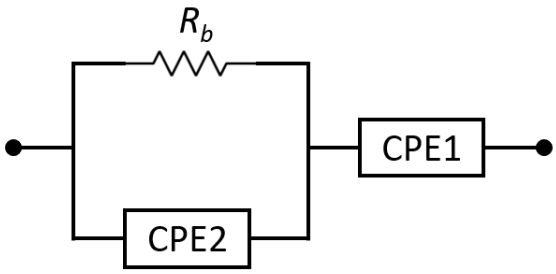

Figure 2. Corresponding electrical equivalent circuit for the Cole-Cole plots in Figure 1.

Table 7. Bulk resistance and conductivity of thin films obtained at room temperature.

Thin film	R_b (Ω)	σ (S/cm)
CMC-PC-LH2	1.71×10^{4}	5.58×10^{-8}
CMC- PC- [Ni(LH2)$_2$]	5.36×10^{3}	7.72×10^{-8}
CMC- PC- [Co(LH2)$_2$]	5.98×10^{2}	9.58×10^{-7}
CMC- PC- [Cu(LH2)$_2$]	2.67×10^{4}	3.10×10^{-8}

Conductivity Studies

Electrochemical impedance spectroscopy was carried out to investigate the conductivity of the thin films. Figure 1 (a)-(d) shows the Cole-Cole plots of the thin films, while their corresponding equivalent circuit model is illustrated in Figure 2. The model consists of a parallel combination of R_b and a constant phase element (CPE1) in series with another, CPE2, representing both the incomplete semicircle and spike of the Cole-Cole plots [25, 26]. Table 7 lists the values for bulk resistance, R_b, and conductivity, σ, obtained at room temperature. The R_b values were retrieved from the *x*-axis intercepts of the Cole-Cole plots.

Generally, it can be observed that the thin films containing metal complexes exhibited higher conductivity compared to the ligands. This can be attributed to the overlapping of the *d* orbital of the metal and π-orbital of the aromatic ring in the ligand, which would increase electron delocalization in the molecule [27].

In addition, the highest conductivity was observed at 9.58×10^{-7} S cm^{-1} for CMC-PC-[Co(LB2)$_2$]. This behaviour is attributed to the variation in the ionic radii of the metals, as the ionic radius of the Co(II) ion is greater than that of the Ni(II) ion, followed by the Cu(II) ion [28]. However, theoretically, conductivity increases with the size of the metal ion as the weaker attraction to the nucleus causes the free electrons to move around more easily [29].

The addition of propylene carbonate (PC) into the polymer is attributed to the increase in conductivity [30]. Plasticizers have various advantages in improving conductivity by increasing the amorphous content of a polymer-salt complex, with ion dissociation polymer electrolytes, which are preferred at higher salt concentrations. Moreover, plasticizers have low viscosity properties which enhance mobility carriers and increase the amorphous content of the plasticized polymer due to their low melting temperature [31]. This amorphous nature results in greater ion diffusion and leads to better conductivity. PC does not supply ions to the polymer electrolyte system, but it facilitates dissociation into ions and reduces its viscosity, resulting in higher ionic mobility. These H^+ ions can hop *via* each coordinating site (oxygen) of the carboxymethyl cellulose, and thus, conduction occurs [32]. In this study, the surface of the thin films appeared to be smooth and flat without signs of brittleness or cracks, indicating that the samples were homogenous and amorphous. The amorphicity of these thin films will be the subject of further research.

CONCLUSION

New thiosemicarbazone derivatives (LH2) and their transition metal complexes were prepared and their postulate structures were characterized by elemental analysis, molar conductance, magnetic susceptibility and UV-Vis. It was found that the LH2 ligand coordinated with metal ions through its azomethine nitrogen and thiolo sulphur atoms. Unfortunately, all

compounds showed low electrical conductivity values, in the range of $9.58 \times 10^{-7} - 7.72 \times 10^{-8}$ S cm^{-1}, due to the semicrystalline nature of the thin films mixed with carboxymethyl cellulose (CMC) and propylene carbonate (PC).

ACKNOWLEDGEMENTS

This work was supported by the Ministry of Higher Education, Malaysia (MOHE) in the form of a Fundamental Research Grant Scheme (Ref: FRGS/1/2020/STG05/UMT/02/2) (FRGS-59620). The authors would also like to thank the Faculty of Science and Marine Environment, Universiti Malaysia Terengganu (UMT) for the use of their research facilities. All the results in this paper have been presented at the International Congress on Pure & Applied Chemistry, Kota Kinabalu (ICPAC Kota Kinabalu 2022) on 22-27 November 2022.

REFERENCES

1. Cao, Y., Li, H., & Yin, A. (2022). A two-dimensional manganese coordination polymer: Crystal structure, proton conductivity and catalytic property. *Inorganica Chimica Acta*, **529**, 120658.

2. Liang, M., Song, Y., Liu, D., Xu, M., Yang, G., Wang, W., Ran, R., Shao, Z. (2022) Magnesium tuned triple conductivity and bifunctionality of $BaCo_{0.4}Fe_{0.4}Zr_{0.1}Y_{0.1}O_3$-δ perovskite towards reversible protonic ceramic electrochemical cells. *Applied Catalysis B: Environmental*, **318**, 121868.

3. Zhou, Y., Xiang, H., Zhu, J. -Y., Shi, L., You, W. -J., Wei, X. -Q., Tian, Z., Shao, D. (2022) Synthesis, structure, magnetism and proton conductivity of a cyanide-bridged Ni(II) Co(III) framework. *Polyhedron*, **228**, 116181.

4. Chu, Z. -T., Li, R. -Y., Zhou, C. -C., Liu, H. -T., Lu, J., Wang, S. -N. & Li, Y. -W. (2021) Two acidic coordination polymers containing uncoordinated carboxyl groups: Syntheses, crystal structures and proton conductivities in Nafion composite membranes. *Journal of Solid State Chemistry*, **295**, 121932.

5. Yu, L., WangFei & ZhangJian (2017) Synthesis, structure and proton conductivity of a metal–organic framework with rich hydrogen-bonds between the layers. *Inorganic Chemistry Communications*, **79**, 37–40.

6. Osman, U., Silvarajoo, S., Kamaruddin, K., Mohamed Tahir, M., & Kwong, H. C. (2021). Ni(II) complex containing a thiosemicarbazone ligand: Synthesis, spectroscopy, single-crystal X-ray crystallographic and conductivity studies. *Journal of Molecular Structure*, **1223**, 128994.

7. Kotian, A., Kumara, K., Kamat, V., Naik, K., Kokare, D., Nevrekar, A., lokanath, N. K., Revankar, V. (2018) p-halo N4-phenyl substituted thiosemicarbazones: Crystal structure, supramolecular architecture, characterization and bio-assay of their Co(III) and Ni(II) complexes. *Journal of Molecular Structure*, **1156**, 115–126.

8. Zahinos, E., Giles, F., Garcia, P. & Calderon, M. (2011) Co(III), Ni(II), Zn(II) and Cd(II) complexes with 2-acetyl-2-thiazoline thiosemicarbazone: Synthesis, characterization, X-ray structures and antibacterial activity. *European Journal of Medicinal Chemistry*, **46**, 150–159.

9. Zangrando, E., Islam, M., Islam A. A., M. -A., Sheikh, M., Tarafder, M., Miyatake, R., Zahan, R., Hossain, M. (2015) Synthesis, characterization and bio-activity of nickel(II) and copper(II) complexes of a bidentate NS Schiff base of S-benzyl dithiocarbazate. *Inorganica Chimica Acta*, **427**, 278–284.

10. Ghosh, B., Adak, P., Naskar, S., Pakhira, B., Mitra, P. & Chattopadhyay, K. S. (2017) Ruthenium(II/III) complexes of redox non-innocent bis(thiosemicarbazone) ligands: Synthesis, X-ray crystal structures, electrochemical, DNA binding and DFT studies. *Polyhedron*, **131**, 74–85.

11. Jayakumar, K., Sithambaresan, M. & Aiswarya, N. (2015) Synthesis and spectral characterization of mono- and binuclear copper(II) complexes derived from 2-benzoylpyridine-N4-methyl-3-thiosemicarbazone: Crystal structure of a novel sulfur bridged copper(II) box-dimer. *Spectrochimica Acta Part A: Molecular and Biomolecular Spectroscopy*, **139**, 28–36.

12. Demirci, T., Guveli, S., Yesilyurt, S., Ozdemir, N. & Ulkuseven, B. (2020) Thiosemicarbazone ligand, nickel(II) and ruthenium(II) complexes based on vitamin B6 vitamer: The synthesis, different coordination behaviors and antioxidant activities. *Inorganica Chimica Acta*, **502**, 119335.

13. Shi, W., Chen, Y., Chen, X., Xie, Z. & Hui, Y. (2016) Simple-structured, hydrazinecarbothioamide derivatived dual-channel optical probe for Hg2+ and Ag+. *Journal of Luminescence*, **174**, 56–62.

14. Pavia, D., Lampman, G., Kriz, G. & Vyvyan, J. (2009) Introduction to Spectroscopy. (fourth edition). Belmont, CA: Cengage Learning.

15. Yousef, T., Gammal, O., Ghazy, S. & Abu El-Reash, G. (2011) Synthesis, spectroscopic characterization, pH-metric and thermal behavior on Co(II) complexes formed with 4-(2-pyridyl)-3-thiosemicarbazide derivatives. *Journal of Molecular Structure*, **1004**, 271–283.

16. Venugopal, R., Sreejith, S. & Kurup, M. P. (2019) Crystallographic, spectroscopic and theoretical investigations on Ni(II) complexes of a tridentate NNS donor thiosemicarbazone. *Polyhedron*, **158**, 398–407.

17. Gaber, M., Fayed, T. & El-Gamil, M. (2018) Structural, thermogravimetric, B3LYP and biological studies on some heterocyclic thiosemicarbazide copper (II) complexes and evaluation of their molecular docking. *Journal of Molecular Structure*, **1151**, 56–72.

18. Ekennia, A., Osowole, A., Olasunkanmi, L., Onwudiwe, D., Olubiyi, O. & Ebenso, E. (2017). Synthesis, characterization, DFT calculations and molecular docking studies of metal (II) complexes. *Journal of Molecular Structure*, **1150**, 279–292.

19. Akbari, A., Ghateazadeh, H., Takjoo, R., Nejad, B., Mehrvar, M. & Mague, J. (2019) Synthesis & crystal structures of four new biochemical active Ni(II) complexes of thiosemicarbazone and isothiosemicarbazone-based ligands: In vitro antimicrobial study. *Journal of Molecular Structure*, **1181**, 287–294.

20. Kumar, L. V. & Nath, G. R. (2019) Synthesis, characterization and biological studies of cobalt(II), nickel(II), copper(II) and zinc(II) complexes of vanillin-4-methyl-4-phenyl-3-thiosemicarbazone. *J. Chem. Sci*, **131**, 76.

21. Fawzy, A., Farghaly, T. A., El-Ghamry, H. & Bawazeer, T. M. (2020) Investigation of the inhibition efficiencies of novel synthesized cobalt complexes of 1,3,4-thiadiazolethiosemicar bazone derivatives for the acidic corrosion of carbon steel. *Journal of Molecular Structure*, **1203**, 127447.

22. Ceylan, B. I. (2021) Oxovanadium(IV) and Nickel(II) complexes obtained from 2,2′-dihydroxy-benzophenone-S-methyl-thiosemicarbazone: Synthesis, characterization, electrochemistry, and antioxidant capability. *Inorganica Chimica Acta*, **517**, 120186.

23. Joseph, J. & Rani, G. B. (2017) Metal based SOD mimetic therapeutic agents: Synthesis, characterization and biochemical studies of metal complexes. *Arabian Journal of Chemistry*, **10**, S1963–S1972.

24. El-Ghamaz, N., Diab, M., El-Sonbati, A. & Salem, O. (2011) D.C. electrical conductivity and conduction mechanism of some azo sulfonyl quinoline ligands and uranyl complexes. *Spectrochimica Acta Part A: Molecular and Biomolecular Spectroscopy*, **83**, 61–66.

25. Zainuddin, N. K. & Samsudin, A. S. (2018) Investigation on the effect of NH4Br at transport properties in k–carrageenanbased biopolymer electrolytes via structural and electrical analysis. *Materials Today Communications*, **14**, 199–209.

26. Ramlli, M. A., Isa, M. I. N. & Kamarudin, K. H. (2022) 2-hydroxyethyl cellulose-ammonium thiocyanate solid biopolymer electrolytes: Ionic conductivity and dielectric studies. *Journal of Sustainability Science and Management*, **17**, 121–132.

27. El-Ghamaz, N., El-Sonbati, A., Diab, M., El-Bindary, A., Mohamed, G. & Morgan, S. (2015) Correlation between ionic radii of metal azodye complexes and electrical conductivity. *Spectrochimica Acta Part A: Molecular and Biomolecular Spectroscopy*, **147**, 200–211.

28. Morgan, S., El-Ghamaz, N. & Diab, M. (2018) Effect of the type of metal on the electrical conductivity and thermal properties of metal complexes: The relation between ionic radius of metal complexes and electrical conductivity. *Journal of Molecular Structure*, **1160**, 227–241.

29. Alothman, A. & Almarhoon, Z. (2020) Nano-sized some transition metal complexes of Schiff base ligand based on 1-aminoquinolin-2(1H)-one. *Journal of Molecular Structure*, **1206**, 127704.

30. Samsudin, A., & Saadiah, M. (2018). Ionic conduction study of enhanced amorphous solid bio-polymer electrolytes based carboxymethyl cellulose doped NH_4Br. *Journal of Non-Crystalline Solids*, **497**, 19–29.

31. Kumar, M., & Sekhon, S. (2002). Role of plasticizer's dielectric constant on conductivity modification of PEO–NH4F polymer electrolytes. *European Polymer Journal*, **38**, 1297–1304.

32. Hema, M., Selvasekerapandian, S., Sakunthala, A., Arunkumar, D., & Nithya, H. (2008). Structural, vibrational and electrical characterization of PVA–NH4Br polymer electrolyte system. *Physica B: Condensed Matter*, **403**, 2740–2747.